Effects of Oxygen Partial Pressure on the Electrical and Optical Properties of Pulsed-Laser-Deposited Sb-Doped SnO_2 Films

Journal of The Electrochemical Society, **153** (10) G922-G925 (2006)
0013-4651/2006/153(10)/G922/4/$20.00 © The Electrochemical Society

Effects of Oxygen Partial Pressure on the Electrical and Optical Properties of Pulsed-Laser-Deposited Sb-Doped SnO_2 Films

Hyun-Gi Hong,[a] June-O Song,[b] Sang-Ho Kim,[a] Takhee Lee,[a] and Tae-Yeon Seong[c,*,z]

[a]*Department of Materials Science and Engineering, Gwangju Institute of Science and Technology, Gwangju 500-712, Korea*
[b]*School of Electric and Computer Engineering, Georgia Institute of Technology, Atlanta, Georgia 30332-0250, USA*
[c]*Department of Materials Science and Engineering, Korea University, Seoul 136-713, Korea*

We have investigated the electrical and optical properties of pulsed-laser-deposited Sb-doped SnO_2 films (250 nm thick) as a function of the oxygen partial pressure. The SnO_2 films were grown on glass substrates using a SnO_2 target containing 5 atom % Sb. The distance between the substrate and the target was 7 cm and working pressure varied from 1.1 to 13.3 Pa. The target was ablated using KrF excimer laser with energy density of 3.75 J/cm^2. It is shown that the electrical and optical properties of the films grown at 480°C with 3000 pulses sensitively depend on the oxygen pressure. The electron concentration is maximum (5.6×10^{20} cm^{-3}) at 4 Pa, the electron mobility is maximum (8.5 cm^2 V^{-1} s^{-1}) at 9.3 Pa, and the resistivity is minimum (2.5×10^{-3} Ω cm) at 4 Pa. The transmittance is shown to depend on the oxygen pressures. X-ray diffraction results show that the crystalline quality of the films becomes improved with decreasing oxygen pressure. It is further shown that the sample grown at 1.1 Pa contains oxygen-deficient phases. The UV absorption edge of the films shifts toward the shorter wavelengths with decreasing oxygen pressure, which is attributed to Burstein–Moss shift.
 [DOI: 10.1149/1.2239989]

Manuscript submitted August 8, 2005; revised manuscript received May 25, 2006. Available electronically August 4, 2006.

Recently transparent conductive oxides (TCOs) have attracted significant interest because of their application in a variety of devices, such as flat-panel displays, electrochromic devices, and light-emitting diodes contacts.[1-3] In particular, the development of TCOs, which have wide bandgaps and thermal stability, is of much importance for the fabrication of short-wavelength optoelectronic devices.[3] Currently, indium tin oxide (ITO) is the most commonly used TCO because it has high conductivity and transmittance. ITO, however, suffers from a few problems, such as thermal instability, electrical degradation caused by hydrogen plasma treatment, and the exhaustion of indium.[1,4,5]

Tin oxide (SnO_2) is an n-type semiconductor having a wide bandgap of 3.6 eV and has been considered as a promising TCO because of its high thermal and chemical stability. Thus, SnO_2 has been used in photovoltaic cells, transparent electrodes, resistive coatings, and gas sensors.[6-9] Doping TCOs with impurities is an efficient and easy way to improve their electrical properties. For example, Sb, In, and F can be used as dopants to produce n-type SnO_2.[6,7,10] SnO_2 films have been synthesized using various deposition techniques, such as sputtering, spray pyrolysis, chemical vapor deposition, sol-gel, evaporation, and pulsed laser deposition (PLD).[10-15] In particular, PLD is advantageous because it generates highly energetic particles, which allows good film quality, congruent evaporation, and good adhesion to substrates, and is a simple deposition technique.[16] Thus, PLD was also used to grow TiO_2 and ITO films.[17-20] In this work, we have investigated the electrical, optical, and structural properties of Sb-doped SnO_2 thin films on glass substrates by PLD as a function of oxygen partial pressure. The results show that the electrical and optical properties of the samples sensitively depend on the oxygen partial pressure. In particular, when the films are grown at 1.1 Pa, oxygen-deficient phases are formed, resulting in the degradation of the electrical and optical properties of the samples.

Experimental

The SnO_2 films (250 nm in thickness) were grown on Corning glass (1737) substrates by PLD using a sintered SnO_2 disk target (1 in. in diam) containing 5 atom % Sb. The glass substrates were ultrasonically cleaned for 10 min using acetone and then rinsed by methanol. After that, the glass substrates were placed on a ceramic heating stage, and the distance between the substrate and the target was kept at 7 cm. Growth chamber was evacuated to 1.3×10^{-4} Pa. Working pressure varied from 1.1 to 13.3 Pa by monitoring oxygen gas from a leak valve. After heating the substrates, the target was ablated using KrF excimer laser (wavelength: 248 nm; pulse width at half maximum: 25 ns) (COMPex 205, Lambda Physik Co.) with an energy density of 3.75 J/cm^2 at a repetition rate of 5 Hz. The electrical properties of the Sb-doped SnO_2 films were characterized by means of Hall measurement method with the Van der Pauw geometry (BIO-RAD HL5500PC) and their optical properties by UV-visible spectrometer (Varian Cary 1E, HP 8452A diode-array spectrometer). X-ray diffraction (XRD, Rigaku Rint 2000 with a Cu Kα radiation) analysis was performed to investigate the structural properties of the Sb-doped SnO_2 films. To characterize the chemical states of the Sb-doped SnO_2 films, X-ray photoelectron spectroscopy (XPS, PHI 5200 model) was carried out using an Al Kα X-ray source in an UHV system with a chamber base pressure of $\sim 1.3 \times 10^{-8}$ Pa. The film thickness was measured by means of field emission scanning electron microscope (Hitachi S-4700) operated at 15 kV.

Results and Discussion

Figure 1 shows the substrate-temperature dependence of the resistivity of the 250 nm thick SnO_2 films, which were grown at 3000 pulses under a working pressure of 4 Pa. As the substrate temperature increases from room temperature to 480°C, the resistivity decreases from 0.135 to 2.51×10^{-3} Ω cm, possibly due to the activation of dopants and the improvement of the crystalline quality of the films. However, when the temperature further increases to 550°C, the resistivity increases slightly and the film exhibits bluish color, indicating a slight degradation of its transparency.

Figure 2 shows the oxygen partial-pressure dependence of the electrical properties of the SnO_2 films that were grown at 480°C with 3000 pulses. As the oxygen partial pressure decreases from 13.3 to 1.1 Pa, the electron concentration (marked a) increases, reaches maximum (5.61×10^{20} cm^{-3}) at 4 Pa, and then decreases. The electron mobility (marked b) increases, reaches maximum (8.5 cm^2 V^{-1} s^{-1}) at 9.3 Pa, and then decreases, as the oxygen pres-

* Electrochemical Society Active Member.
z E-mail: tyseong@korea.ac.kr

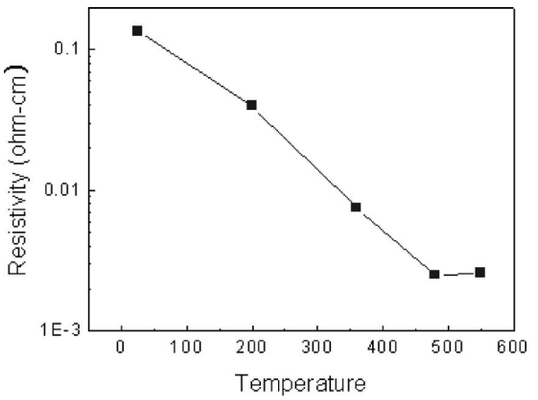

Figure 1. The substrate-temperature dependence of the resistivity of the 250 nm thick SnO_2 films that were grown at 3000 pulses under a working pressure of 4 Pa.

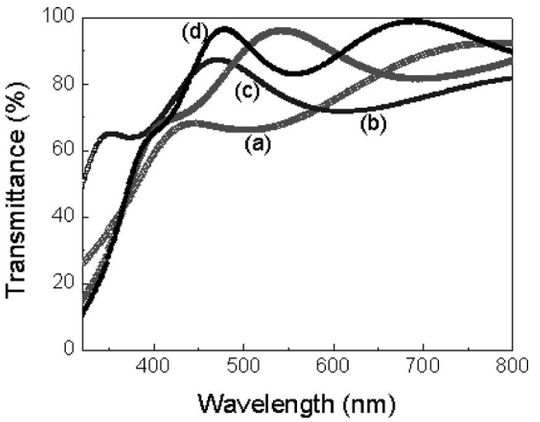

Figure 3. The transmittance of the SnO_2 films that were grown at 480°C with 3000 pulses under the oxygen partial pressure of (a) 1.1, (b) 4, (c) 9.3, and (d) 13.3 Pa.

sure increases. As for the resistivity (marked c), it decreases, reaches minimum (2.5×10^{-3} Ω cm) at 4 Pa, and then increases with increasing oxygen partial pressure. The samples grown at oxygen partial pressures lower than 1.1 Pa yielded insulating characteristics.

Figure 3 shows the transmittance of the SnO_2 films that were grown at 480°C with 3000 pulses as a function of the oxygen partial pressure. The transmittance is dependent on the oxygen partial pressure. For example, the transmittance at wavelength of 405 nm is 61, 70, 67, and 66% for the samples grown at oxygen pressures of 1.1, 4, 9.3, and 13.3 Pa, respectively. It is worth noting that the transmittance of the sample grown at 4 Pa is about 65% at 350 nm. In particular, absorption data in between 320 and 450 nm that were obtained from the same samples of Fig. 3 are shown in Fig. 4. Except for the sample grown at 1.1 Pa, the UV absorption edge shifts toward the shorter wavelengths with decreasing oxygen partial pressure, as expected from the transmittance results (Fig. 3).

Figure 5 shows the XRD patterns of the SnO_2 films that were grown at 480°C with 3000 pulses under different oxygen partial pressures. As the oxygen partial pressure decreases, the crystalline quality of the films becomes improved. For the sample grown at 1.1 Pa, there is an additional broad peak, corresponding to SnO (110) tetragonal phase, and oxygen-deficient phase peaks (as circled) (e.g., Sn_3O_4 and SnO).[21]

To further investigate the presence of the oxygen-deficient phase, XPS examination was made of the SnO_2 films grown at 480°C with 3000 pulses under the oxygen pressures of 1.1 and 13.3 Pa. For the sample grown at 13.3 Pa (Fig. 6a), the XPS spectra reveal the typical oxidation state of Sn, i.e., SnO_2.[22] The [O]/[Sn] atomic ratio was calculated using an equation given as[22]

$$C_{Sn} = \{(I_{Sn3d}/S_{Sn3d})/[(I_{Sn3d}/S_{Sn3d}) + (I_{O1s}/S_{O1s})]\}$$

where C_{Sn} is the atomic percentage of Sn, $I_{Sn\ 3d}$ is the peak intensity of Sn $3d_{5/2}$, $S_{Sn\ 3d}$ is the sensitivity factor (4.095) of Sn $3d_{5/2}$, $I_{O\ 1s}$ is the peak intensity of O 1s, and $S_{O\ 1s}$ is the sensitivity factor (0.711) of O 1s.[22] The calculation showed that the SnO_2 film grown at 13.3 Pa has an [O]/[Sn] atomic ratio of 1.82, while the sample grown at 1.1 Pa has a ratio of 1.7. The atomic ratios lower than 2 indicate that the sample contains a lot of oxygen-related defects, such as oxygen vacancies.

As the oxygen pressure decreased, the carrier concentration increased and reached maximum at 4 Pa, and then decreased (Fig. 1). The increasing behavior could be attributed to the increase of oxygen vacancies, serving as donors. For the sample grown at 1.1 Pa, however, the reduction could be related to the formation of highly resistive oxygen-deficient phases (SnO and Sn_3O_4) embedded in the SnO_2 film, as noted by the XRD and XPS results (Fig. 5 and 6). The inclusion of such resistive phases degrades the electrical properties of the films. The electron mobility increased with increasing oxygen partial pressure (from 1.1 to 9.3 Pa). This behavior could be related

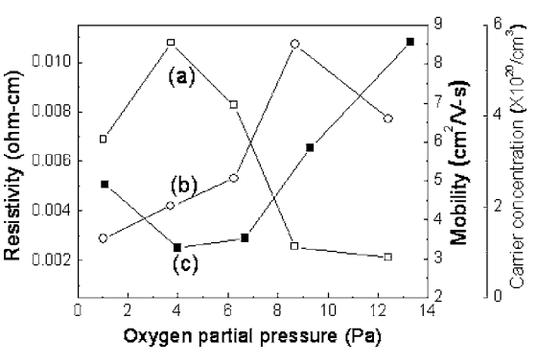

Figure 2. The oxygen partial-pressure dependence of (a) the carrier concentration, (b) the mobility, and (c) the resistivity of the SnO_2 films that were grown at 480°C with 3000 pulses.

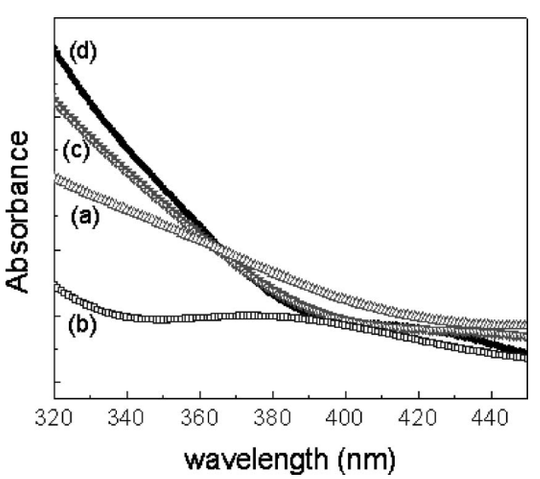

Figure 4. Absorption data inbetween 320 and 450 nm, which were grown at 480°C with 3000 pulses under the oxygen partial pressure of (a) 1.1, (b) 4, (c) 9.3, and (d) 13.3 Pa.

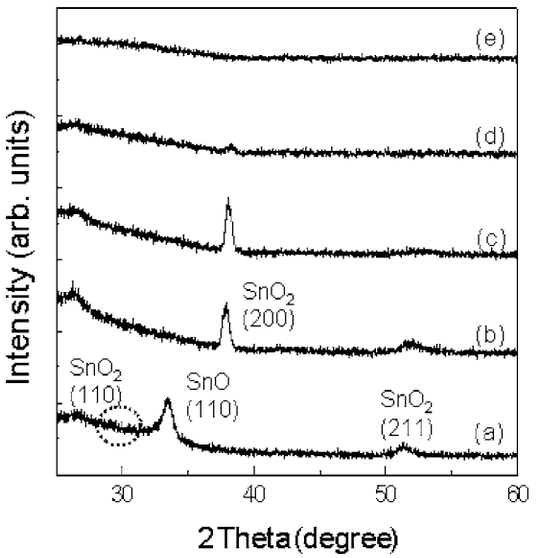

Figure 5. The XRD data of the SnO_2 films that were grown at 480°C with 3000 pulses under (a) 1.1, (b) 4, (c) 6.7, (d) 9.3, and (e) 13.3 Pa.

to the formation of defects such as oxygen vacancy and oxygen-deficient phases at lower oxygen pressures. The slightly degraded mobility at 13.3 Pa could be attributed to the poor crystalline quality of the films.[17] During PLD growth under high oxygen pressures, a plume is confined, resulting in the reduction of the kinetic energy of the evaporated particles from the target. Thus, it would be difficult for them to reach appropriate nucleation sites on the substrate under the high oxygen pressure, leading to the growth of poor-crystalline films.

The shift of the absorption edge (Fig. 4) could be explained in terms of Burstein–Moss shift.[23,24] This phenomena could occur if the electron concentration would exceed Mott critical density (N), which is defined as $N = (0.25m_c^* e^2/\varepsilon_o \hbar^2)^3$, where m_c^* is the conduction band effective mass and ε_o is the permittivity of free space.[25] For the SnO_2, this can occur when the electron concentration exceeds about 10^{18} cm^{-3}. Thus, as the carrier concentration increases, their conduction band is partially filled and consequently the optical bandgap, which is given by the energy separation between the valence band maximum and the lowest unfilled level in the conduction band, is expanded, leading to the shift of the absorption edge toward the higher energy-side, as shown in Fig. 4. The SnO_2 film grown at 1.1 Pa exhibited yellowish color with lower transmittance than compared with the other samples. This could be explained in terms of the formation of the oxygen-deficient phases.[26] It was known that the Sn_3O_4 and SnO films have bandgap energy in the range 2.5–3 eV, which is lower than that of the SnO_2.

To investigate if the Sb-doped SnO_2 p-type contact layer is suitable for devices, near-UV (405 nm) GaN-based light-emitting diodes (LEDs) were fabricated using the Sb-doped SnO_2 p-contact electrodes. The LED mesa structure (300×300 μm) was comprised of a GaN buffer layer, n-GaN, an InGaN/GaN multiquantum well-active layer, and p-GaN. The SnO_2 film was deposited by PLD at oxygen pressure of 4 Pa and annealed at 480°C for 1 min in air. For comparison, the electrical behavior of LEDs made with conventional Ni(5 nm)/Au(5 nm) p-type contact layers were also characterized. Figure 7 shows the current–voltage (I–V) and light-output characteristics of LEDs fabricated with different p-type electrodes. The LED with the SnO_2 gives a slightly higher I–V characteristic than that of the LED with the Ni/Au (Fig. 7a). However, the light-output characteristic was dramatically improved (Fig. 7b). For example, the LED with the SnO_2 shows the enhancement of output power by 68% compared with the one with the Ni/Au at an injection

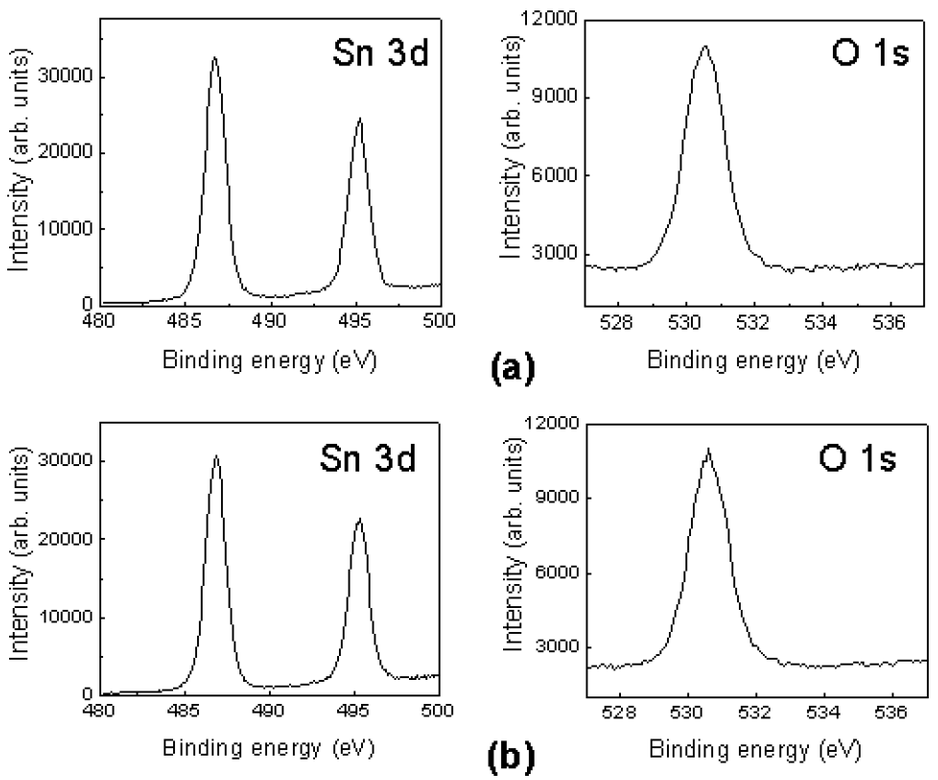

Figure 6. XPS spectra obtained from the SnO_2 films grown at 480°C with 3000 pulses under the oxygen pressures of (a) 1.1 and (b) 13.3 Pa.

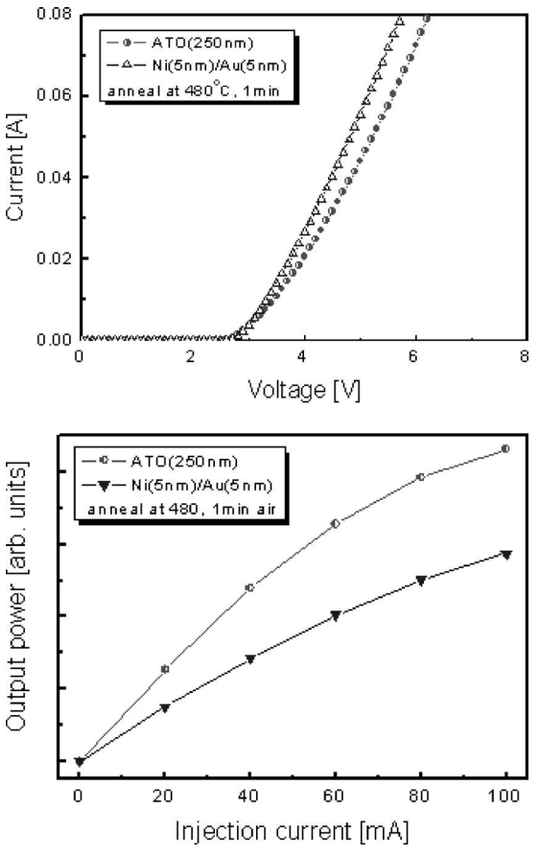

Figure 7. (a) The I–V and (b) light-output characteristics of LEDs fabricated with different p-type electrodes.

current of 20 mA. This can be explained in terms of the higher transmittance of the SnO_2 films as compared with the Ni/Au contact.

Conclusion

The 250 nm thick Sb-doped SnO_2 films were grown by PLD and their electrical and optical properties were investigated as a function of the oxygen partial pressure. It was shown that the electrical and optical properties of the films grown at 480°C with 3000 pulses are sensitively dependent on the oxygen partial pressure. The films grown at 480°C with 3000 pulses under 4 Pa produced the optimum properties with the electron concentration of 5.61×10^{20} cm^{-3}, the resistivity of 2.5×10^{-3} Ω cm, and transmittance of 70% at wavelength of 405 nm. However, the growth at a very low pressure of 1.1 Pa led to the formation of oxygen deficient phases, degrading the film quality. These results show that the PLD-grown Sb-doped SnO_2 films have potential as a TCO for use in the fabrication of short-wavelength optoelectronic devices.

Korea University assisted in meeting the publication costs of this article.

References

1. D. S. Ginley and C. Bright, *Mater. Res. Soc. Symp. Proc.*, **25**, 15 (2000).
2. H. L. Hartnagel, A. L. Dawar, A. K. Jain, and C. Jagadish, *Semiconducting Transparent Thin Films*, Institute of Physics Publishing, London, (1995).
3. J. O. Song, K. K. Kim, S. J. Park, and T.-Y. Seong, *Appl. Phys. Lett.*, **83**, 479 (2003).
4. R. Banerjee, S. Ray, N. Basu, A. K. Batabyal, and A. K. Barua, *J. Appl. Phys.*, **62**, 912 (1987).
5. T. J. Coutts, D. L. Young, X. Li, W. P. Mulligan, and X. Wu, *J. Vac. Sci. Technol. A*, **18**, 2646 (2000).
6. W. A. Badawy, H. H. Afify, and E. M. Elgiar, *J. Electrochem. Soc.*, **137**, 1592 (1990).
7. A. K. Abass and M. T. Mohammad, *J. Appl. Phys.*, **59**, 1641 (1986).
8. J. C. Manifacier, *Thin Solid Films*, **90**, 297 (1982).
9. W. Gopel and K. D. Schierbaum, *Sens. Actuators B*, **26**, 1 (1995).
10. H. Kim and A. Pique, *Appl. Phys. Lett.*, **84**, 218 (2004).
11. H. Ma, X. Hao, J. Ma, Y. Yang, J. Huang, D. Zhang, and X. Xu, *Appl. Surf. Sci.*, **191**, 313 (2002).
12. K. Y. Rajpure, M. N. Kusumade, M. N. Neumann-Spallart, and C. H. Bhosale, *Mater. Chem. Phys.*, **64**, 184 (2000).
13. L. Bruno, C. Pijolat, and R. Lalauze, *Sens. Actuators B*, **18**, 195 (1994).
14. C. Terrier, J. P. Chatelon, and J. A. Roger, *Thin Solid Films*, **295**, 95 (1997).
15. M. Mizuhashi, *J. Non-Cryst. Solids*, **38**, 329 (1980).
16. D. B. Chrisey and G. K. Hubler, *Pulsed Laser Deposition of Thin Films*, John Wiley & Sons, New York (1994).
17. J.-H. Kim, S. Lee, and H.-S. Im, *Appl. Phys. A*, **69**, S629 (1999).
18. J.-H. Kim, S. Lee, and H.-S. Im, *Appl. Surf. Sci.*, **151**, 6 (1999).
19. S. H. Kim, N.-M. Park, T. Kim, and G. Y. Sung, *Thin Solid Films*, **475**, 262 (2005).
20. H. Izumi, F. O. Adurodija, T. Kaneyoshi, T. Ishihara, H. Yoshioka, and M. Motoyama, *J. Appl. Phys.*, **91**, 1213 (2002).
21. R. Dolbec, M. A. El Khakani, A. M. Serventi, M. Trudeau, and R. G. Saint-Jacques, *Thin Solid Films*, **419**, 230 (2002).
22. J. F. Moulder, W. F. Stickle, P. E. Sobol, and K. D. Bomben, *Handbook of X-Ray Photoelectron Spectroscopy*, Physical Electronics, Inc., Eden Prairie, MN (1995).
23. E. Burstein, *Phys. Rev.*, **93**, 632 (1954).
24. T. S. Moss, *Proc. Phys. Soc. London*, **67**, 775 (1964).
25. N. F. Mott, *Metal Insulator Transitions*, Taylor and Francis, London (1974).
26. S. Muranaka, Y. Bando, and T. Takada, *Thin Solid Films*, **86**, 11 (1981).